Experimental characterization of a CuAg alloy for thermo-mechanical applications: non-linear plasticity models and low-cycle fatigue curves

D. Benasciutti[a,]*, F. De Bona[b], L. Moro[b], J. Srnec Novak[b]

[a]Department of Engineering, University of Ferrara, via Saragat 1, Ferrara 44122, Italy
[b]Politechnic Department of Engineering and Architecture (DPIA), University of Udine, via delle Scienze 208, Udine 33100, Italy

Abstract

The cyclic response and low-cycle fatigue strength of a CuAg0.1 alloy for thermo-mechanical applications are investigated by isothermal strain-controlled fatigue tests at three temperature levels (room temperature, 250°C, 300°C). Both cyclic and stabilized stress-strain responses are used for identifying the material parameters of non-linear kinematic (Armstrong-Frederick, Chaboche) and isotropic models. The identified material parameters are used in numerically simulated cycles, which are successfully compared to experiments. Linear regression analysis of experimental fatigue data allows the "mean" low-cycle fatigue curves to be estimated. Approximate statistical methods are finally adopted to evaluate the design low-cycle fatigue curves at prescribed failure probability and confidence levels.

Keywords: CuAg alloy, plasticity models, cyclic hardening, low-cycle fatigue.

1. Introduction

Copper alloys have an optimal combination of high conductivity and good mechanical properties, which makes these materials suitable in thermo-mechanical applications in which components are subjected to high thermal flux

---

* Corresponding author. Tel.: +39 (0)532-974976; fax: +39 (0)532-974870.
  E-mail address: denis.benasciutti@unife.it

combined to mechanical loads. An example in continuous casting plants is a mold (or crystallizer), which is a long (~1m) hollow component where the molten steel starts to solidify. Owing to the high temperatures of the molten steel, the mold is subjected to a high thermal flux − also varying over time (due to plant switch on/off) − which may cause a network of thermal cracks to appear on the inner surface.

In the design phase, finite element modeling can profitably be used for simulating the mold thermo-mechanical response and to compute stresses and strains, which, combined with fatigue curves, allow the mold service life to be estimated. Numerical modeling requires suitable plasticity models, calibrated on experimental data. Conventional molds are usually made by CuAg, CuCrZr, or sometimes CuNiBe alloys [1]. While thermo-physical and mechanical properties in the literature mainly refer to CuCrZr alloys, data for CuAg alloys are far more scarce [1].

Aiming to provide a contribution, this work will experimentally characterize a CuAg0.1 alloy for thermo-mechanical applications by using low-cycle fatigue tests at three different temperatures (room, 250 °C, 300 °C). Stress-strain data recorded in each test are used for identifying parameters of non-linear kinematic and isotropic plasticity models. Numerical simulations using the identified material parameters are next compared to experimental cyclic responses.

Experimental data are finally used for estimating the low-cycle fatigue curves by regression analysis and further re-analyzed by approximate statistical methods to evaluate design fatigue curves at prescribed levels of failure probability and confidence. The results of this extensive experimental characterization could be used both for numerically simulating the cyclic plasticity response and for estimating the service life of components in CuAg alloy that are subjected to thermo-mechanical loads.

Nomenclature

b	speed of stabilization	β	confidence level
c	fatigue ductility exponent	γ	non-linear recovery parameter
C	initial hardening modulus	$\varepsilon_{a,el}$	elastic strain amplitude
D	ductility	$\varepsilon_{a,pl}$	plastic strain amplitude
e	fatigue strength exponent	$\varepsilon_{a,tot}$	total strain amplitude
E	Young's modulus	$d\boldsymbol{\varepsilon}_{pl}$	plastic strain rate tensor
N	number of cycles	$\varepsilon_{pl,acc}$	accumulated plastic strain
N_f	number of cycles to failure	ε'_f	fatigue ductility coefficient
$2N_f$	number of reversals to failure	σ_{y0}	initial yield stress
R	drag stress - isotropic variable	σ_{ys}	cyclic (saturated) yield stress
R_∞	saturation value	σ_a	stress amplitude
s	standard deviation	σ'_f	fatigue strength coefficient
$\boldsymbol{S}$	deviatoric stress tensor	$\sigma_{max,1}$	maximum stress in 1st cycle
$\boldsymbol{X}$	back stress (kinematic) tensor	$\sigma_{max,s}$	maximum stress in stabilized cycle
α	failure probability	σ_{uts}	ultimate tensile strength

2. Non-linear hardening models: theoretical background

The yield surface can be represented by a combined kinematic and isotropic model as [2]:

$$\sqrt{\frac{3}{2}(\boldsymbol{S}-\boldsymbol{X}):(\boldsymbol{S}-\boldsymbol{X})}-R-\sigma_{y0}=0 \tag{1}$$

where $\boldsymbol{S}$ is the deviatoric stress tensor, $\boldsymbol{X}$ is the kinematic tensor (back stress), R is the isotropic variable (drag stress), σ_{y0} is the initial yield stress (in absence of plastic deformation). The back stress controls the translation of the yield surface (kinematic model), whereas the isotropic variable R controls the homothetic expansion (isotropic model) of the yield surface. Kinematic and isotropic models are implemented in commercial finite element codes and allow

simulating the elasto-plastic response of materials subjected to cyclic loadings, especially in steel-making components [3-7].

The literature provides several theories for kinematic and isotropic models. In the non-linear kinematic Armstrong-Frederick (AF) model, for example, the increment of the back stress tensor is related to the increment of both plastic strain tensor $d\varepsilon_{pl}$ and accumulated plastic strain $\varepsilon_{pl,acc}$ [2]:

$$dX = \frac{2}{3}Cd\varepsilon_{pl} - \gamma X d\varepsilon_{pl,acc} \tag{2}$$

where C is the initial hardening modulus and γ is the non-linear recovery parameter that controls the decrease rate of the hardening modulus as plastic strain accumulates. For uniaxial loading, Eq. (2) yields [2]:

$$X = \nu\frac{C}{\gamma} + \left(X_0 - \nu\frac{C}{\gamma}\right)\exp\left[-\nu\gamma\left(\varepsilon_{pl} - \varepsilon_{pl,0}\right)\right] \tag{3}$$

in which $\nu=\pm 1$ defines the load direction (tension or compression), $\varepsilon_{pl,0}$ and X_0 are the initial values of plastic strain and back stress, respectively, at the beginning of each loading branch. In a stabilized cycle, the stress amplitude σ_a, the saturated yield stress σ_{ys} and the plastic strain amplitude $\varepsilon_{a,pl}$ are related by [2]:

$$\sigma_a = \sigma_{ys} + \frac{C}{\gamma}\tanh\left(\gamma\varepsilon_{a,pl}\right) \tag{4}$$

The Chaboche model is obtained by superimposing several AF models [2]:

$$X = \sum_{i=1}^{n}X_i \quad ; \quad dX_i = \frac{2}{3}C_i\,d\varepsilon_{pl} - \gamma_i\,X_i d\varepsilon_{pl,acc} \quad \rightarrow \quad \sigma_a = \sigma_{ys} + \sum_i\frac{C_i}{\gamma_i}\tanh\left(\gamma_i\,\varepsilon_{a,pl}\right) \tag{5}$$

The non-linear isotropic model is governed by the following equation [2]:

$$dR = b(R_\infty - R)d\varepsilon_{pl,acc} \tag{6}$$

where R_∞ is the saturated drag stress, b is the parameter that controls the speed of hardening ($R_\infty>0$) or softening ($R_\infty<0$). Integration of Eq. (6) for uniaxial loading gives an expression that links drag stress to accumulated plastic strain [2]:

$$R = R_\infty\left[1 - \exp\left(-b\varepsilon_{pl,acc}\right)\right] \tag{7}$$

For cyclic loading, the evolution of R can also be correlated to the change of maximum stress $\sigma_{max,i}$ in the Nth cycle, relative to the maximum stress in the first cycle, $\sigma_{max,1}$, and in the stabilized cycle, $\sigma_{max,s}$ [2]:

$$\frac{\sigma_{max,i} - \sigma_{max,1}}{\sigma_{max,s} - \sigma_{max,1}} \cong \frac{R}{R_\infty} = 1 - e^{-b\varepsilon_{pl,acc}} \tag{8}$$

In strain-controlled loading, the accumulated plastic strain after N cycles is $\varepsilon_{pl,acc} \approx 2\Delta\varepsilon_{pl}N$, where $\Delta\varepsilon_{pl}=2\varepsilon_{a,pl}$ is the plastic strain range (twice the amplitude) in one cycle. The non-linear isotropic model in Eq. (8) assumes that the change of maximum stress σ_{max} in cyclic hardening/softening only depends on the amount of accumulated plastic strain $\varepsilon_{pl,acc}$, independently of the actual value of plastic strain amplitude $\varepsilon_{a,pl}$. In a combined model, the kinematic

and isotropic models sum up and, in uniaxial loading, the maximum stress at a certain level of accumulated plastic strain $\varepsilon_{pl,acc}$ is $\sigma_{max}(\varepsilon_{pl,acc})=\sigma_{y0}+X(\varepsilon_{pl,acc})+R(\varepsilon_{pl,acc})$.

3. Plasticity models: identifying parameters from experimental data

3.1. Experimental tests

Low-cycle fatigue (LCF) tests were carried out on a CuAg0.1 alloy, classified in ASTM B 124 standard [8]. Fatigue tests were performed on un-notched cylindrical specimens at three temperature levels: room (20 ^{o}C), 250 ^{o}C, 300 ^{o}C. Experimental tests applied strain-controlled cycles with fully reversed (R_ε=-1) triangular waveform and strain rate 0.01 s^{-1}. Room temperature tests used a servo-hydraulic Instron-Schenck machine with nominal force ±250 kN and mechanical grips. High temperature tests used an Instron machine with nominal force ±100 kN and water cooled grips, where specimens were induction heated (coil). In all tests, elongation of samples was measured by extensometers. Tests were interrupted before specimen complete failure. The number of cycles to failure N_f was conventionally defined when the maximal stress decreased by 80% from its initial value. Additional information about experimental testing can be found in [9].

3.2. Identification of material parameters

Young's modulus E and initial yield stress σ_{y0} were identified first, as they allowed the elastic strain $\varepsilon_{el}=\sigma/E$ and plastic strain $\varepsilon_{pl}=\varepsilon-\varepsilon_{el}$ to be computed from the total strain ε and axial stress σ recorded in loading cycles. The Young's modulus was determined on the straight upward portion of the first cycle. Subsequently, the initial yield stress σ_{y0} was identified on the tensile portion of the first loading cycle, while the cyclic (saturated) yield stress σ_{ys} was measured on the stabilized stress-strain cycle (approximately at half of the total number of cycles to failure).

Table 1. Material parameters estimated from experimental data.

Temp. [°C]	E [MPa]	σ_{y0} [MPa]	Kinematic model						Isotropic model	
			C_1	γ_1	C_2	γ_2	C_3	γ_3	R_∞	b
20	119080	130	40240	2611	36700	2612	17330	342.1	-75.7	2.352
200	106600	113	39740	1550	18060	1532	6503	302.7	-80.2	3.894
300	103800	110	28600	1052	11850	599.8	1142	517.6	-76.6	5.293

Parameters of plasticity models (kinematic and isotropic) were estimated separately and sequentially. In fact, the kinematic model stabilizes after a few cycles [2] and the change of maximum stress during cyclic loading is essentially controlled by the isotropic model. On the other hand, the isotropic model gives a negligible increment of maximum stress in the first cycle, due to the small value of accumulated plastic strain associated to a small speed of stabilization for the CuAg alloy (small b parameter, see Table 1).
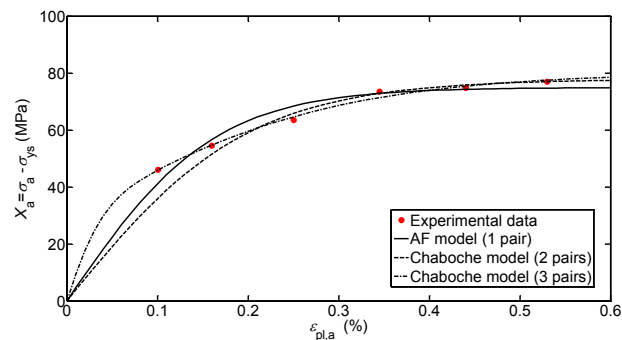

Fig. 1. Kinematic model calibrated on experimental data at room temperature.

Kinematic variables were determined by considering several stabilized cycles at different values of strain amplitude. For each stabilized cycle, the amplitude of back stress $X_a = \sigma_a - \sigma_{vs}$ was calculated from the values of stress amplitude σ_a and the cyclic yield stress σ_{vs} estimated before. Fig. 1 displays an example for room temperature data. The lines represent the "best fitted" models with one, two or three pairs of kinematic parameters (C_i, γ_i) – the three-pair model gave the lowest fitting error .
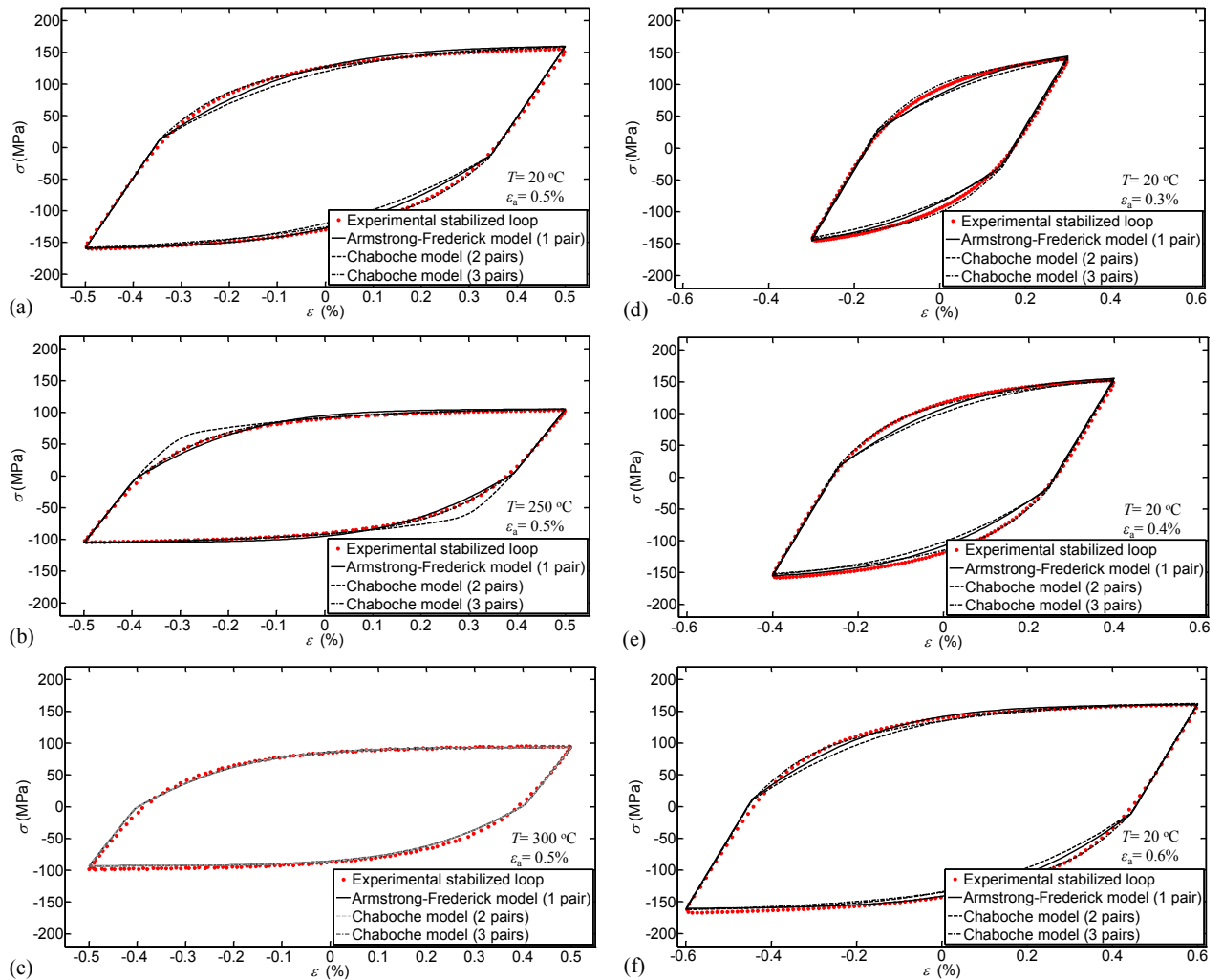

Fig. 2. Comparison between experimental vs. simulated cycles: (a)-(c) same strain amplitude, different temperatures; (d)-(f) same temperature, different strain amplitudes.

Fig. 2 compares the experimental cycles to numerically simulated cycles obtained by a kinematic model implementing the parameters (C_i, γ_i) identified before. The three-pair model always gives the best agreement to experiments, both for cycles at same strain amplitude and different temperature (room, 250 °C, 300 °C) and for cycles at same temperature and different strain amplitudes. Table 1 summarizes the parameters estimated at each temperature.

Isotropic variables (R_∞, b) were estimated next. Fig. 3(a) illustrates the evolution of the maximum stress $\sigma_{max,i}$ at each loading cycle N, for cycles at different values of total strain amplitude $\varepsilon_{a,tot}$. The decreasing trend confirms a softening behaviour for the CuAg alloy. The saturated stress $R_\infty = \sigma_{max,1} - \sigma_{max,s}$ is the difference between the maximum stress in the first cycle, $\sigma_{max,1}$, and in the stabilized cycle, $\sigma_{max,s}$.
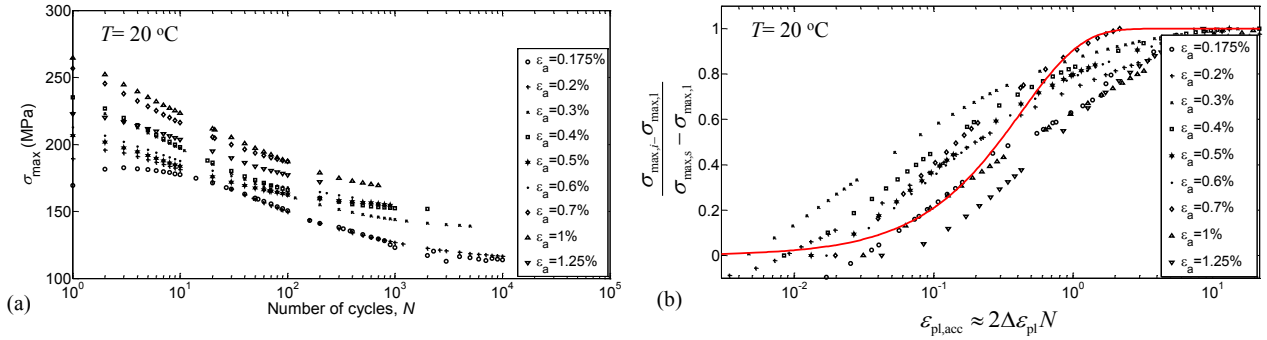
Fig. 3. (a) Maximum stress vs. number of cycles; (b) "best fitting" of isotropic model. Room temperature data.

The values $\sigma_{max,i}$, $\sigma_{max,1}$, $\sigma_{max,s}$ are then combined to plot, in Fig. 3(b), the left hand side of Eq. (8) against the number of cycles N, for different values of strain amplitude $\varepsilon_{a,tot}$. Fig. 3(b) points out a marked dependence on the strain amplitude, which actually contradicts the hypothesis behind the isotropic model. This dependence, also observed in [10] for a nickel-based superalloy, explains the poor fitting observed in Fig. 3(b). Parameter b was finally estimated by calibrating Eq. (8) to the experimental points in Fig. 3(b).

Finally, Fig. 4 compares the experimental cycles to simulated cycles obtained by a combined kinematic and isotropic model, whose parameters (see Table 1) were estimated previously. Fig. 4 refers to 50 cycles at a strain amplitude $\varepsilon_{a,tot}$=0.5%, at room temperature.

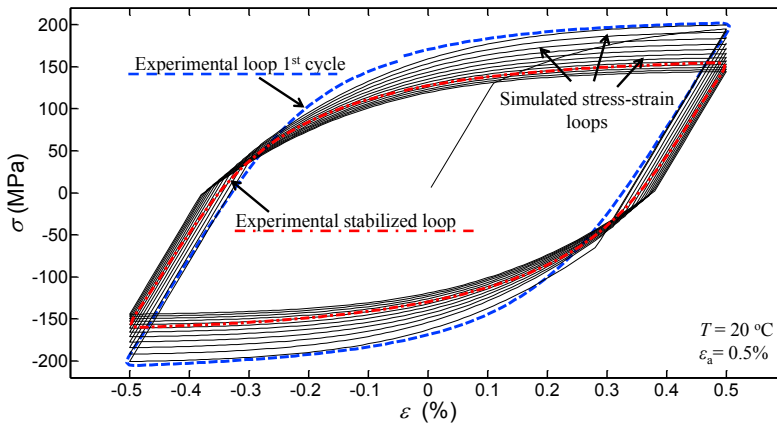

Fig. 4. Comparison between experiments and cycles simulated by a combined model.

4. Low-cycle fatigue curves

Experimental low-cycle fatigue data were used to estimate the Manson-Coffin equation [11]:

$$\varepsilon_{a,tot} = \varepsilon_{a,el} + \varepsilon_{a,pl} = \frac{\sigma'_f}{E}\left(2N_f\right)^e + \varepsilon'_f\left(2N_f\right)^c \tag{9}$$

where $\varepsilon_{a,tot}$ is the total strain amplitude (sum of elastic $\varepsilon_{a,el}$ and plastic $\varepsilon_{a,pl}$ strain amplitudes), $2N_f$ is the number of reversals to failure, whereas other symbols are: σ'_f = fatigue strength coefficient, ε'_f = fatigue ductility coefficient, e, c =exponents.

To calibrate the parameters of Eq. (9) on experimental data, a regression analysis has to be performed separately for the elastic and plastic strain contributions. To this purpose, a regression model $y=A+Bx+\delta$ is used, where

$x=\log(\varepsilon_a)$, $y=\log(2N_f)$ are the transformed variables (obviously, $\varepsilon_a=\varepsilon_{a,el}$ and $\varepsilon_a= \varepsilon_{a,pl}$ for elastic and plastic components), whereas δ is a Gaussian random variable with zero mean value and constant standard deviation s ("homoscedastic" model), which allows the regression model to quantify the statistical scatter of fatigue life $2N_f$.
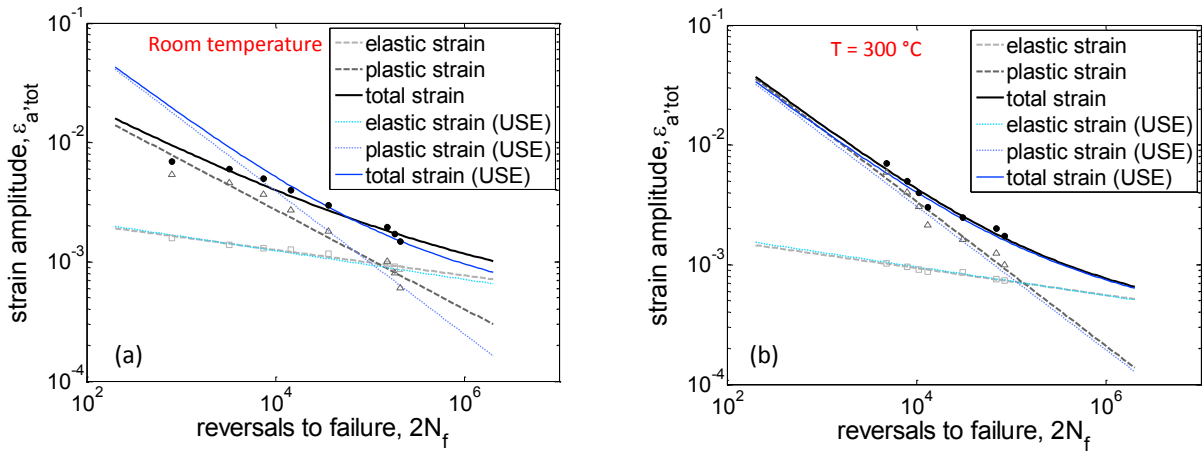

Fig. 5. Low-cycles fatigue tests at room temperature and 300 °C: experiments, regression lines and "Universal Slopes Equation".

Linear regression analysis provides a set of expressions (e.g. see [11]) that permit the estimators $\hat{A}$, $\hat{B}$, $\hat{s}$, and therefore the "mean" strength curve $\hat{y} = \log(2\hat{N}_f) = \hat{A} + \hat{B}x$, to be estimated from n experimental points (x_i, y_i), $i=1,\dots,n$. The parameters of the "mean" Manson-Coffin curve are then obtained directly by anti-transforming the regression estimators [12]:

$$\frac{\hat{\sigma}'_f}{E} = 10^{\left(-\hat{A}_{el}/\hat{B}_{el}\right)} \quad , \quad \hat{e} = \frac{1}{\hat{B}_{el}} \qquad ; \qquad \hat{\varepsilon}'_f = 10^{\left(-\hat{A}_{pl}/\hat{B}_{pl}\right)} \quad , \quad \hat{c} = \frac{1}{\hat{B}_{pl}} \tag{10}$$

where subscripts "el" and "pl" refer to the elastic and plastic components, respectively. The low-cycle fatigue curve in total strain amplitude is obtained by summing up the equations of elastic and plastic strain components. In Fig. 5, the "mean" low-cycle fatigue curve is compared with experimental tests at room temperature and 300 °C (elastic, plastic and total strain contributions are shown).

4.1. Approximate low-cycle fatigue curves from monotonic tensile properties

Low-cycle fatigue tests are generally costly and time-consuming. Simplified methods for estimating fatigue curves from monotonic tensile properties are particularly useful, especially in industry or at early design phases. A noteworthy example of simplified method is the "*Universal Slopes Equation*" (USE) proposed by Manson [11,13]:

$$\Delta\varepsilon_{tot} = \Delta\varepsilon_{el} + \Delta\varepsilon_{pl} = 3.5\left(\frac{\sigma_{uts}}{E}\right)N_f^{-0.12} + D^{0.6}N_f^{-0.6} \tag{11}$$

where σ_{uts} is the tensile strength, D the ductility depending on percent necking $Z\%$, whereas fixed slopes -0.12 and -0.6 are assumed for all materials (note that the equation refers to strain range). Equation (11) represents a "mean" curve; its parameters must be estimated at the considered service temperature. Although originally calibrated on low-cycle fatigue data for ferrous and non-ferrous alloys (e.g. steel, silver, magnesium, titanium, aluminum), Eq. (11) is here applied to the CuAg alloy considered in this work. Fig. 5 compares the USE in Eq. (11) with the experimental data at room temperature and 300 °C. A very good agreement is observed at 300 °C (likewise at 250 °C), whereas a slightly less satisfactory fitting concerns room temperature data (see Fig. 5(a)).

4.2. Statistical analysis and design curves

The "mean" low-cycle fatigue curve $\hat{y} = \hat{A} + \hat{B}x$ is defined for a failure probability α=50%, which is too high to be accepted in design. A suitably higher safety margin (i.e. a much lower probability) has to be specified, so that a design curve (shifted on the left side of the "mean" curve) is obtained:

$$\hat{y}_{\mathrm{d}} = \hat{y} - k_{\alpha,\beta,n,x} \cdot \hat{s} \tag{12}$$

where $k_{\alpha,\beta,n,x}$ is a statistical factor depending on the failure probability α and confidence level β (if required), on the sample size n (i.e. number of fatigue tests) and on the particular strain amplitude x=log(ε_{a}) at which life $\hat{y}_{\mathrm{d}}$=log($2N_{\mathrm{f,d}}$) is computed.

In the literature, several methods are available to evaluate the design curves (i.e. the value of $k_{\alpha,\beta,n,x}$ and the percentile $\hat{y}_{\mathrm{d}}$): i) deterministic method ("2 or 3 sigma"), ii) statistical method, which can be further divided into methods for evaluating the confidence interval, tolerance interval and prediction interval [14].

In the most general case in which $k_{\alpha,\beta,n,x}$ explicitly depends on the amplitude x, the design curve has a "hyperbolic" shape (it is not a straight line). Approximate statistical methods are nevertheless available to evaluate a constant factor $k_{\alpha,\beta,n}$ that is independent of x. In this case, the design curve is straight and shifted on the left side of the "mean", according to the expression:

$$\hat{y}_{\mathrm{d}} = \left(\hat{A} - k_{\alpha,\beta,n} \cdot \hat{s}\right) + \hat{B}x \tag{13}$$

where $\hat{A}_{\alpha,\beta} = \hat{A} - k_{\alpha,\beta,n} \cdot \hat{s}$ is a new constant that is function of failure probability α (survival probability is $1-\alpha$) and confidence β. These approximate methods are particularly useful, as they permit the parameters σ'_{f}, $\varepsilon'_{\mathrm{f}}$ of the Manson-Coffin curves to be obtained according to the following quite simple expressions:

$$\left(\frac{\hat{\sigma}'_{\mathrm{f}}}{E}\right)_{\mathrm{d}} = 10^{\left[-\left(\hat{A}_{\mathrm{el}} - k\hat{s}\right)/\hat{B}_{\mathrm{el}}\right]} \qquad \left(\hat{\varepsilon}'_{\mathrm{f}}\right)_{\mathrm{d}} = 10^{\left[-\left(\hat{A}_{\mathrm{pl}} - k\hat{s}\right)/\hat{B}_{\mathrm{pl}}\right]} \tag{14}$$

The slopes of the elastic and plastic strain components are equal to the exponents e, c resulting from the linear regression analysis (the design curve is indeed a straight line translated with respect to the regression line). In the next paragraphs particular attention is addressed on the approximate methods that give a constant value of k and therefore permit the Manson-Coffin design curve to be defined according to Eq. (14).

4.2.1. Deterministic method ("2 or 3 sigma")

According to this approach, the regression estimators coincide with the "real" parameters: $\hat{A} = A$, $\hat{B} = B$, $\hat{s} = s$. The variable y is thus Gaussian with mean value $\hat{y}$ and standard deviation s. By using the cumulative probability function $\Phi(z)$ for the standard Gaussian variable z, it is possible to evaluate $k_{\mathrm{det}} = z_{1-\alpha} = \Phi^{-1}(1-\alpha)$ for a given survival probability $1-\alpha$. As an example, for a failure probability α=1% it follows: $k_{\mathrm{det}} = z_{0.99} = 2.3263$. This approach is not conservative, as it neglects the statistical uncertainty of $\hat{A}$, $\hat{B}$ and $\hat{s}$ [14].

4.2.2. One-side tolerance interval method

A tolerance interval defines a region enclosing a percentage of the population of a given random variable. Calculating the tolerance interval is trivial for a Gaussian distribution with known mean value μ and standard deviation s. As an example, 95% of a Gaussian distribution falls within the two-side interval $\mu \pm 1.96s$, where $z_{0.975} = \Phi^{-1}(0.975) = 1.96$.

If the Gaussian variable y=log($2N_{\mathrm{f}}$) is considered, the value $\hat{y}_{\mathrm{d}}$ defined from the design curve Eq. (12) identifies a one-side interval $y \leq \hat{y}_{\mathrm{d}}$, which encloses a percentage α of the values y. For the variable y, however, the regression analysis only gives the estimators (and not the "true" values) of both the mean value $\hat{A} + \hat{B}x$ and the standard

deviation $\hat{s}$. It follows that a statistical uncertainty is introduced, which does not allow the function $\Phi(z)$ to be used for evaluating factor k (as in the "deterministic method").

A different approach taking into account also the confidence β of the estimates is therefore necessary to evaluate k. The goal is to determine a value $k_{\alpha,\beta,n}$ that defines the lower bound $\hat{y}_d$ of the one-side tolerance interval $y \leq \hat{y}_d$, which is expected to contain (with a predetermined confidence β) a percentage α of the values y. Factor $k_{\alpha,\beta,n}$ depends on the failure probability α, on the confidence level β and on the size n of the statistical sample. For a Gaussian distribution, the values of $k_{\alpha,\beta,n}$ are tabulated [14]. As an example, if $n=7$, $\alpha=1\%$, $\beta=90\%$, it is $k_{\alpha,\beta,n}=3.9720$. The design curve $\hat{y}_d = \hat{y} - k_{\alpha,\beta,n} \cdot \hat{s}$ obtained by this method ensures that in the long run, $100\beta\%$ of times, failures at $\hat{y} \leq \hat{y}_d$ occur with probability α.

The tolerance interval method provides a constant $k_{\alpha,\beta,n}$ along the whole amplitude interval x and it thus returns a straight design line. The method is, however, correct only if a single random variable is considered. In the regression case (two variables), the method is only approximate, as it neglects the statistical uncertainty of regression estimators [14].

If the tolerance interval method is applied to linear regression ("Owen's method"), the $k_{\alpha,\beta,n,x}$ factor also depends on the strain level x and the design curve is not straight any more. This approach raises some practical difficulties, yet. A possible approximation ("approximate Owen's method") consists in considering a value $(k_{\alpha,\beta,n})_{app}$ constant on the whole x interval. It is therefore possible to define the design curve as the straight line $\hat{y}_d = \hat{y} - (k_{\alpha,\beta,n})_{app} \cdot \hat{s}$. Omitting the theoretical details (see [15]), the values of $(k_{\alpha,\beta,n})_{app}$ are tabulated in [16] for different values of n, α and β (in [15] some values are not correct, yet). As an example, given $n=7$, $\alpha=1\%$, $\beta=90\%$, it is $(k_{\alpha,\beta,n})_{app}=4.3187$.

4.2.3. Prediction interval method

A prediction interval defines a region where a future value of a random variable is likely to fall with a certain probability. In this case, the uncertainty of the future observation has to be added to that of estimators $\hat{A}$, $\hat{B}$, $\hat{s}$.

In the expression of the prediction interval (see [17]), $k_{\alpha,n,x}$ is a "t-Student" random variable that depends on the failure probability α, on the strain amplitude x and on the sample size n. As a result, the design curve is not straight. In [17] an approximate method (called "*equivalent prediction interval*", EPI) was proposed to evaluate a constant $(k_{\alpha,n})_{EPI}$ factor. The method basically assumes that the Gaussian variable y has a constant standard deviation $\sigma_0 = \hat{s} \cdot g_{\alpha,n}$, calculated by introducing a correction factor $g_{\alpha,n}$ (which assesses the uncertainty of the estimators $\hat{A}$, $\hat{B}$, $\hat{s}$). The following expressions (for $6 \leq n \leq 50$, $0.01 \leq \alpha \leq 0.15$) were proposed in [17]:

$$g_{\alpha,n} = \exp\left[\Lambda(\alpha)\left\{\ln n\right\}^{-\Psi(\alpha)}\right] \quad ; \qquad \Lambda(\alpha) = 1.56\left[\tanh^{-1}(1-\alpha)\right]^{1.12} \quad ; \quad \Psi(\alpha) = 3.32 - 1.7\alpha \tag{15}$$

Once the value of σ_0 is determined, the design curve is $\hat{y}_{EPI} = \hat{y} - (k_{det} \cdot g_{\alpha,n})\hat{s}$. It is finally possible to define $k_{EPI} = k_{det} \cdot g_{\alpha,n}$, where k_{det} is the factor evaluated by the deterministic method (see Sec. 4.2.1). As an example, given $n=7$, $\alpha=1\%$, it is $k_{EPI}=3.8924$.

4.2.4. Results

As an example, Fig. 6 plots the Manson-Coffin design curves (only plastic strain component) estimated by the previously proposed statistical methods applied to experimental data at 300 °C ($n=7$), for a failure probability $\alpha=1\%$ and confidence $\beta=90\%$. The analysis was also performed for the elastic part, although not shown here. Table 2 summarizes the obtained values of the parameters σ'_f, ε'_f, e, c. The Manson-Coffin design curve in elastic $\varepsilon_{a,el}$, plastic $\varepsilon_{a,pl}$ and total $\varepsilon_{a,tot}$ strain amplitude is obtained by introducing in Eq.(9) the values of Table 2.

For both elastic and plastic strain components, the tolerance interval method ("approximate Owen's method") provides the most conservative curve (i.e. that laying on the most left-side from the regression line), whereas both the one-side tolerance interval approach and the EPI approach provide overlapped lines, slightly shifted to the right. The deterministic method gives, instead, the less conservative design curve, i.e. that closest to the regression line.
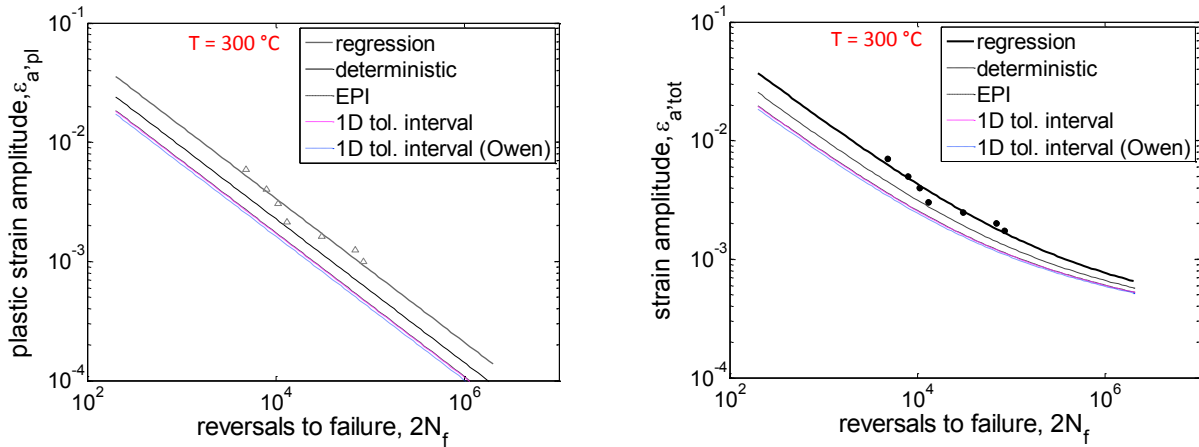
Fig. 6. Design curves for data at 300 °C, referred to failure probability α=1% and confidence β=90%, expressed as a function of the amplitude of: (a) plastic strain; (b) total strain.

Besides the low-cycle design curves, in design it is also of interest to know the strain amplitude $(\varepsilon_{a,tot})_d$ for a prescribed number of reversals to failure $(2N_f)_d$. The last column of Table 2 presents the design values of strain amplitude for $(2N_f)_d=2\cdot10^5$. As already observed, the assessment based on the tolerance interval method for the regression case ("approximate Owen's method") gives the most conservative value, 30% lower than the value from the "mean" (regression) line.

Table 2. Parameters of Manson-Coffin equation ("mean" and design curve) for experimental data at 300 °C.

Method	k	σ'_f/E	e	ε'_f	c	$(\varepsilon_{tot,a})_d$ [b]
linear regression (α=1%)[a]	-	0.00244	-0.1125	0.57468	-0.6035	0.00122
deterministic method (α=1%)	2.3263	0.00227	-0.1125	0.38764	-0.6035	0.00099
EPI (α=1%, n=7)	3.8924	0.00217	-0.1125	0.29738	-0.6035	0.00088
1D tolerance interval (α=1%, β=90%, n=7)	3.9720	0.00216	-0.1125	0.29340	-0.6035	0.00087
1D tolerance interval (Owen) (α=1%, β=90%, n=7)	4.3187	0.00214	-0.1125	0.27667	-0.6035	0.00085

[a] α= failure probability; β=confidence; n=sample size
[b] values referred to design life $(2N_f)_d=2\cdot10^5$

5. Conclusions

This work deals with an experimental characterization of a CuAg0.1 alloy used in thermo-mechanical applications. Results of low-cycle fatigue tests at three different temperatures (room temperature, 250 °C, 300 °C) were considered. The experimental cyclic response was used to identify the parameters of non-linear kinematic and isotropic plasticity models. The Chaboche model (three pairs of C, γ) has shown the best agreement with measured stabilized stress-strain cycles. The calibration of the non-linear isotropic model was then performed by considering the whole evolution of cycles, which showed a softening behavior. The statistical analysis of low-cycle fatigue data was finally performed to estimate the "mean" Manson-Coffin curve and also the design curves (at given failure probability and confidence) by approximate statistical methods that make use of simple analytical formula for evaluating curve parameters. Compared to the "mean" fatigue line, the design strain amplitude was shown to decrease up to 30%.

References

[1] G. Li, B.G. Thomas, J.F. Stubbins, Modeling creep and fatigue of copper alloys, Metall. Mater. Trans. A. 31A (2000) 2491–2502.

[2] J. Lemaitre, J.L. Chaboche, Mechanics of solid materials, Cambridge University Press, Cambridge, 1990.

[3] D. Benasciutti, On thermal stress and fatigue life evaluation in work rolls of hot rolling mill, J. Strain Anal. Eng. Des. 47(5) (2012) 297–312.

[4] D. Benasciutti, F. De Bona, M.Gh. Munteanu, An harmonic 1D-element for non linear analysis of axisymmetric structures: The case of hot rolling, Proc. of 1st Pan-American Congress on Computational Mechanics (PANACM 2015) and 11th Argentine Congress on Computational Mechanics (MECOM 2015), Buenos Aires, 27-29 April 2015, 1566–1577.

[5] D. Benasciutti, F. De Bona, M.Gh. Munteanu, A harmonic one-dimensional element for non-linear thermo-mechanical analysis of axisymmetric structures under asymmetric loads: The case of hot strip rolling, J. Strain Anal. Eng. Des. 51(7) (2016) 518–531.

[6] J. Srnec Novak, A. Stanojevic, D. Benasciutti, F. De Bona, P. Huter (2015), Thermo-mechanical finite element simulation and fatigue life assessment of a copper mould for continuous casting of steel, Procedia Engineering 133 (2015) 688–697.

[7] L. Moro, D. Benasciutti, F. De Bona, M.Gh. Munteanu, Simplified numerical approach for the thermo-mechanical analysis of steelmaking components under cyclic loading: An anode for electric arc furnace. Ironmak. Steelmak. (2017), doi: 10.1080/03019233.2017.1339482.

[8] ASTM B 124 - B 124M, Standard Specification for Copper and Copper Alloy Forging Rod, Bar, and Shapes, 2008.

[9] J. Srnec Novak, D. Benasciutti, F. De Bona, A. Stanojevic, A. De Luca, Y. Raffaglio, Estimation of material parameters in nonlinear hardening plasticity models and strain life curves for CuAg alloy, IOP Conf. Series: Materials Science and Engineering 119 (2016) 012020.

[10] L.G. Zhao, B. Tong B, B. Vermeulen, J. Byrne, On the uniaxial mechanical behaviour of an advanced nickel base superalloy at high temperature. Mech. Mater. 33 (2001) 593-600.

[11] S.S. Manson, G.R. Halford, Fatigue and durability of structural materials. Materials Park, OH: ASM International, 2006.

[12] ASTM E739-10 (2015), Standard practice for statistical analysis of linear or linearized stress-life (S-N) and strain-life (ε-N) fatigue data.

[13] S.S. Manson. Fatigue, A complex subject – Some simple approximations. Exp. Mech. 5(4) (1965) 193–226.

[14] C.L. Shen, P.H. Wirsching, G.T. Cashman, Design curve to characterize fatigue strength. J. Eng. Mater. Technol.-Trans. ASME 118 (1996) 535–541.

[15] C.R. Williams, Y-L. Lee, J.T. Rilly, A practical method for statistical analysis of strain-life fatigue data. Int. J. Fatigue 25 (2003) 427–36.

[16] Y.-L. Lee, J. Pan, R.B. Hathaway, M.E. Barkey, Fatigue testing and analysis (theory and practice). Elsevier Butterworth-Heinemann, 2005.

[17] P.H. Wirsching, S. Hsieh, Linear model in probabilistic fatigue design. J. Eng. Mech. Div.-ASCE 106(EM6) (1980) 1265–78.